ENVIRONMENTAL RESEARCH
LETTERS

LETTER

Water scarcity challenges across urban regions with expanding irrigation

Lokendra S Rathore[1], **Mukesh Kumar**[1,*], **Naota Hanasaki**[2], **Mesfin M Mekonnen**[1] and **Pushpendra Raghav**[1]

[1] Civil, Construction and Environmental Engineering, The University of Alabama, Tuscaloosa, AL, United States of America
[2] National Institute for Environmental Studies, Ibaraki, Japan
[*] Author to whom any correspondence should be addressed.

E-mail: mkumar4@eng.ua.edu

Keywords: irrigation expansion, blue water availability, blue water scarcity

Supplementary material for this article is available online

OPEN ACCESS

RECEIVED
1 September 2023

REVISED
17 November 2023

ACCEPTED FOR PUBLICATION
20 December 2023

PUBLISHED
11 January 2024

Abstract

Irrigation expansion is often posed as a promising option to enhance food security. Here, we assess the influence of expansion of irrigation, primarily in rural areas of the contiguous United States (CONUS), on the intensification and spatial proliferation of freshwater scarcity. Results show rain-fed to irrigation-fed (RFtoIF) transition will result in an additional 169.6 million hectares or 22% of the total CONUS land area facing moderate or severe water scarcity. Analysis of just the 53 large urban clusters with 146 million residents shows that the transition will result in 97 million urban population facing water scarcity for at least one month per year on average versus 82 million before the irrigation expansion. Notably, none of the six large urban regions facing an increase in scarcity with RFtoIF transition are located in arid regions in part because the magnitude of impact is dependent on multiple factors including local water demand, abstractions in the river upstream, and the buffering capacity of ancillary water sources to cities. For these reasons, areas with higher population and industrialization also generally experience a relatively smaller change in scarcity than regions with lower water demand. While the exact magnitude of impacts are subject to simulation uncertainties despite efforts to exercise due diligence, the study unambiguously underscores the need for strategies aimed at boosting crop productivity to incorporate the effects on water availability throughout the entire extent of the flow networks, instead of solely focusing on the local level. The results further highlight that if irrigation expansion is poorly managed, it may increase urban water scarcity, thus also possibly increasing the likelihood of water conflict between urban and rural areas.

1. Introduction

Increasing population, dietary changes, and growing per capita income are elevating global food demand [1–7]. Considering 2005 as base year, estimates indicate that crop production needs to be roughly doubled to satisfy the food demand by 2050 [2]. Achieving this ambitious goal is further complicated by the impacts of climate change, which affect food production and pose challenges to global food security [8, 9]. Several strategies are being practiced or explored to increase the crop productivity and making it more resilient [10–17]. Among these, a prominent option is through the expansion and intensification of irrigated agriculture [18–20]. Irrigation can substantially increase crop yield, and reduce the risks from droughts [21, 22]. Given that the share of irrigated cropland in the US was only 16% in 2005, even though it accounted for 44% of the total crop production [23], there is a potential to significantly increase crop productivity through the transition of rainfed agriculture to irrigation-fed in the US. Recognizing this opportunity, several recent studies have explored its potential implications. For example, it was recently reported that transitioning 26% of the current global rainfed land to irrigation-fed can

feed an extra 2.8 billion population [18]. Despite its potential, rain-fed to irrigation-fed (RFtoIF) transition may not always be sustainable, especially if the transition is poorly managed. The irrigation expansion may cause river water depletion, groundwater depletion, and pose a threat to the aquatic ecosystem, thus resulting in freshwater scarcity [24–27].

In this study, we assess the potential impacts of RFtoIF transition of US croplands on blue water scarcity in the contiguous United States (CONUS). Given that RFtoIF transition is expected to increase the water demand for agriculture in the rural areas, our hypothesis is that it may have an impact on the water supply of domestic and industrial sectors in the urban areas. Here we specifically assess the proliferation of blue water scarcity, taking into account both the surface and renewable groundwater availability, in large urban clusters (LUCs) (see section 2.1) due to increased agricultural water use from RFtoIF transition in regions which are largely concentrated in rural areas. In contrast to a majority of the past studies concerned with water scarcity evaluations [28–36], and much like a few selected studies [37–39], here we explicitly consider the role of water transfer to urban areas from 316 surface water withdrawal points. While this study shares certain similarities with previous studies by Flörke *et al* [38] and He *et al* [37], which discussed future increases in water scarcity in urban areas with higher intensity of irrigation intensification in existing irrigated regions, this study, unlike the previous ones, assesses the changes in scarcity also due to spatial expansion of irrigation in previously non-irrigated areas. Furthermore, this study provides additional insights into the causes of why certain regions are more or less susceptible to the impacts of irrigation expansion on water scarcity vis-à-vis their water demand and buffering capacity of ancillary water sources. The need for this evaluation is timely especially given the latent potential for irrigation expansion in central and eastern United States, where several regions have already experienced more than 100% increase in irrigation expansion just within 20 years period [40].

2. Methods

2.1. Definition of urban and rural areas

The US Census Bureau delineates geographic areas identifying them as urban or rural. Urban areas represent densely developed aggregations of census blocks, and usually encompass residential, commercial, and other non-residential land uses. Areas not qualifying as urban are coined as rural. Here, the urban-rural area information is obtained from US Census Bureau as TIGER/line Shapefile [41].

In this study, we assess the impact of RFtoIF in 53 large urban clusters (also referred as LUCs henceforth) which are spread over around 11.9 million hectares and populate around 146 million people. The choice of these LUCs is partly motivated by their significant populace, exceeding 750 000, and also due to the availability of comprehensive surface water withdrawal points data for them [39]. Population information for urban regions is obtained from Gridded Population of the World (GPW), SEDAC [42].

2.2. Assessment of blue and green water scarcity

Green water scarcity is assessed using the GWS index which captures the fraction of crop water requirement that is not met by green water, and is obtained as the ratio of monthly irrigation water demand (=crop water requirement—green water use) and crop water requirement [43]. Green water refers to the rainwater and soil moisture consumed by crops. GWS is calculated at monthly resolution using

$$\mathrm{GWS} = \frac{\mathrm{CWR} - \mathrm{CWSG}}{\mathrm{CWR}} \tag{1}$$

where, CWR is crop water requirement or the amount of water required by a crop to grow optimally, and CWSG is the crop water supply from green water. CWR and CWSG for a given month are calculated by summing daily PET and AET for the month, respectively. GWS is calculated for rainfed crops, therefore, water-limited AET that is solely due to precipitation is used here (see supplementary information for more detail). A region is considered green water scarce if CWSG $<$ 0.9 CWR or in other words, GWS $>$ 0.1 based on Rosa *et al* [43].

Blue water scarcity in this study is quantified using the cumulative abstraction to demand (CAD) metric, which is the ratio of water abstraction to water demand [24]. CAD is calculated at a monthly time step as the ratio of monthly water abstraction to the demand of all the sectors in the grid cell. Here water abstraction corresponds to abstracted water from both surface and subsurface sources, while the water demand quantifies the total water needed to satisfy the demands of agricultural, domestic, and industrial sectors [44]. When water abstraction in a region is less than the water demand, CAD falls below unity. Generally, CAD $<$ 1 indicates a water shortage, and an alternative source of water is needed to alleviate water scarcity. Smaller is the CAD value, more severe is the scarcity. A low, moderate, high, and severe blue water scarcity corresponds to 0.8 $<$ CAD $\leqslant$ 0.99, 0.5 $<$ CAD $\leqslant$ 0.8, 0.3 $<$ CAD $\leqslant$ 0.5, and CAD $\leqslant$ 0.3, respectively. The water scarcity classification thresholds using CAD are consistent with the other widely used water scarcity indexes- water withdrawal to availability and water availability per capita [45]. Herein, all reported results regarding the regions that face scarcity correspond to CAD $\leqslant$ 0.8, which indicates a moderate to high blue water scarcity, unless explicitly stated otherwise.

2.3. H08 model simulations

To assess the impacts of RFtoIF transition on blue water scarcity, a global hydrological model, H08 [44], is used to simulate monthly water availability over the CONUS at a spatial resolution of 5 × 5 arcmin. Two scenario simulations are performed. Scenario S1 represents the status quo during 1996–2005, a period around which most of the input data for H08 are available at continental scale (e.g. crop area fraction for 19 crops [46], irrigated area fraction [47], etc). Scenario S2 simulates the transition of all rain-fed croplands that experience green water scarcity, to irrigation-fed.

The H08 consists of six submodels named land surface, river routing, crop growth, water abstraction, environmental flow, and reservoir operations. H08 was run at daily time intervals and a spatial resolution of 5-arcmin over the period 1996–2005 for the CONUS. All submodels of H08 are coupled to obtain monthly blue water demand for agricultural, industrial, and domestic sectors, and blue water availability in each cell. Blue water demand is satisfied by varied surface and groundwater sources. Surface water is supplied by rivers, canals, reservoirs, and desalination plants while groundwater is supplied from renewable and nonrenewable groundwater resources. The municipal sector is given priority in water supply, followed by the industrial and agricultural sectors, respectively. Daily meteorological forcing data of precipitation, wind speed, air temperature, air pressure, specific humidity, and longwave and shortwave radiation were obtained from NLDAS [48] at 0.125°, hourly, and downscaled at 5 arc min, daily. Additional non-meteorological input data including irrigated area- area equipped for irrigation and area actually irrigated [47], cropland area [49], crop area fraction and spatial distribution of 18 selected crops [46], and water withdrawal for domestic and industrial sectors (FAO [50]) were obtained for the year circa 2000. Other relevant data for H08, including parameterizations, were directly obtained based on Hanasaki *et al* [51] The environmental flow requirements (EFRs) are determined using Shirakawa's algorithm in which all grids are classified (dry, wet, and stable) based on the monthly minimum and maximum streamflow [52].

The model divides a grid cell into four subcells for the irrigated first-crop area, irrigated second-crop area, rainfed area, and no crop area. Irrigated areas are assumed to support a maximum of two crops, a major crop or the first-crop and a secondary crop as the second-crop. The model estimates daily irrigation water requirements using meteorological forcing, crop and agricultural information (crop intensity, crop type, irrigation efficiency, etc). Irrigation is applied to the crops to maintain 75% soil saturation. Annual national industrial and municipal water requirements are obtained from the AQUASTAT database [50] and spatially interpolated at 5 arc min according to the population density [42].

H08 incorporates two types of reservoirs, large and medium-sized. Large reservoirs have a catchment area of more than 5000 km^2 and are located on the main river streams and can control the flow. The medium size reservoirs are generally located in the tributaries and act as tank storage, it stores the water until the storage capacity is reached. Any additional water than storage capacity is released to downstream.

The canal water supply system in the H08 enables the grids to transfer water to large distances. H08 considers two types of aqueducts characterized as explicit and implicit. Explicit canals are those that are physically constructed and can be validated by literature, while implicit canals are based on the assumption that the river water is shared with the first neighboring cell. Implicit canals help prevent the artificial gap in water availability for the cells nearby rivers. Due to the unavailability of the continental scale data of explicit canals, the model may underestimate the water abstraction, especially in urban areas. This is alleviated to some extent by the use of city water map data that provides information on the water sources for 53 cities in the US [39]. Large cities abstract water from urban withdrawal points (groundwater, surface water, and desalination plants), some of them are located around a few hundred kilometers away from the cities. Urban water withdrawal point information was implemented in H08 as canal origins.

For both scenarios, S1 and S2, the model [44] allocates water to a grid according to the water demand and availability at the source of water. The available water in any grid is the sum of runoff generated in the grid, renewable groundwater reserve, canal water abstraction, water abstraction from reservoirs, and water released from upstream grids after fulfilling their all-sectoral demands to the grid under consideration. The model also accounts for EFRs [53] as an additional demand, while estimating the blue water scarcity.

2.4. Assessment of intensification and proliferation of blue water scarcity

The total water demand and abstraction in a LUC is calculated by summing the demand of all LUC grids. The ratio between total monthly water abstraction, both from surface and groundwater, to demand summed over all LUC grids represents CAD for LUCs

$$\mathrm{CAD}_{\mathrm{LUC},m} = \frac{\mathrm{TA}_{\mathrm{LUC},m}}{\mathrm{TD}_{\mathrm{LUC},\,m}} \tag{2}$$

where $\mathrm{TA}_{\mathrm{LUC},m}$ and $\mathrm{TD}_{\mathrm{LUC},m}$ are total monthly water abstraction and demand in LUC grids, respectively, calculated by summing daily industrial and domestic water abstraction and demand. We did not consider the agricultural water demand in LUC grids due to the presence of small fraction of irrigated croplands in suburban areas. Urban water withdrawal points serve

additional source of water abstraction for LUCs. It is assumed that if an urban water withdrawal point is designated to supply water to a city, all the city's grids can abstract water from it based on their demand.

In this study, the intensification of water scarcity is defined as the increase in intensity of blue water scarcity following RFtoIF transition, i.e. areas facing CAD $\leqslant$ 0.99 being lower CAD in S2 than in S1. Spatial proliferation of blue water scarcity indicates expansion of areas (or model cells, used interchangeably henceforth) that do not face water scarcity to begin with, i.e. CAD $>$ 0.99 in S1, but do so following RFtoIF transition, i.e. CAD $\leqslant$ 0.99 in S2.

3. Results

3.1. RFtoIF transition's impact on sectoral water use and blue water scarcity

In scenario S1, more than 72.8% of the total cropland area or 82.5% of the total rainfed cropland faces green water scarcity for at least one month in a year (figure S1). This is consistent with previous studies where 70% of the cropland area was reported to be facing green water scarcity in the CONUS [43] during the same period [54]. To assess the reliability of our model outputs, we further evaluate the model's performance by comparing simulated runoff with the composite runoff generated by Fekete et al., 2002 [54]. The Nash-Sutcliffe Efficiency (NSE) for this comparison yielded a value of 0.69, indicating a robust association between the model results and composite runoff data over the CONUS. Spatially, the GWS magnitude for any given month generally increases with the monthly aridity index (PET/P) (figure S2). Areas facing green water scarcity for at least one month a year on average in S1, are considered for RFtoIF transition in S2 (figure S3).

Given that freshwater is predominantly shared among agricultural, domestic, and industrial sectors, RFtoIF transition alters water availability, and consequently, water withdrawal by all three sectors. Specifically, irrigation expansion causes an increase in annual average agricultural water demand over the simulation period, with total water withdrawal increasing from 318 million m^3 per day to 1119 million m^3 per day after the RFtoIF transition (figure S4). The largest increase takes place in the summer (table S2). Notably, the increase in agricultural water use results in less water available for industrial and domestic water use, resulting in a reduction from 600 million m^3 per day to 587 million m^3 per day.

Next, we assess the average monthly blue water scarcity for both scenarios. The difference in CAD, after and before the RFtoIF transition shows the impact of transition on blue water scarcity (figure 1). The land area facing at least a moderate annual average blue water scarcity (CAD $\leqslant$ 0.8) increases from 71.5 million ha ($\sim$9.33% of the total land area in CONUS) to 241.08 million ha ($\sim$31.45% of the total land area), i.e. an increase of 169.6 million ha, after RFtoIF transition (see definitions of blue water scarcity severities in section 2.1). The spatial distribution of blue water scarcity varies monthly, and peaks in spring and summer largely because of the increased water demand during this period. The impact is maximum during the month of August, when the land area facing moderate blue water scarcity increases from 68.6 million ha ($\sim$9% of the total land area in CONUS) to 228.7 million ha ($\sim$30% of the total land area) after RFtoIF transition. In S1, around 27% and 66% of the CONUS face blue water scarcity that is at least moderate (CAD $\leqslant$ 0.8) and low (CAD $\leqslant$ 0.99) in intensity for at least one month, respectively. The corresponding values increase to 49% and 76% after the RFtoIF transition. The scarcity intensification is largest in High Plains, with Texas, Kansas, and Nebraska experiencing intensification in the majority of months. Significant expansion is also experienced in the eastern US, which has low or no water scarcity in scenario S1. California, Oklahoma, Iowa, Indiana, South Dakota, North Dakota, Minnesota, Illinois, and Missouri observe the spatial proliferation of blue water scarcity, mainly in the summer (figure 1). The somewhat conspicuous reduction of CAD in North Dakota in winter is due to a reduction in water availability for industrial and domestic sectors, which in turn is a result of upstream usage of water for irrigation of winter crops in Montana following RFtoIF transition. Notably, the water reduction in North Dakota is small but the change in CAD is high due to the small water demand. Some areas of Mississippi and Arkansas that contribute to the lower Mississippi river basin also show an increase in blue water scarcity in the summer after the RFtoIF transition.

RFtoIF transition is expected to generally increase blue water scarcity in areas undergoing transition because of the extra water usage in irrigation. The aggravated blue water scarcity in the transitioned area indicates that existing renewable water resources (i.e. the river discharge or reservoirs) and water transportation infrastructure (i.e. implicit and explicit aqueducts, and urban water withdrawal points, (see section 2.3)) are inadequate for fulfilling the increased water demand due to RFtoIF transition. Notably, the RFtoIF transition also causes a rise in monthly blue water scarcity in the areas untouched by the transition. This is because an increase in agricultural water withdrawal from surface water sources due to irrigation expansion in upstream areas leads to a reduction in water flow in river channels, and hence less water availability in receiving lakes and reservoirs. Notably, the average annual surface and groundwater use for irrigation increases from 162 and 156 million m^3 per day to 517.8 and 601 million m^3 per day after RFtoIF transition, respectively.

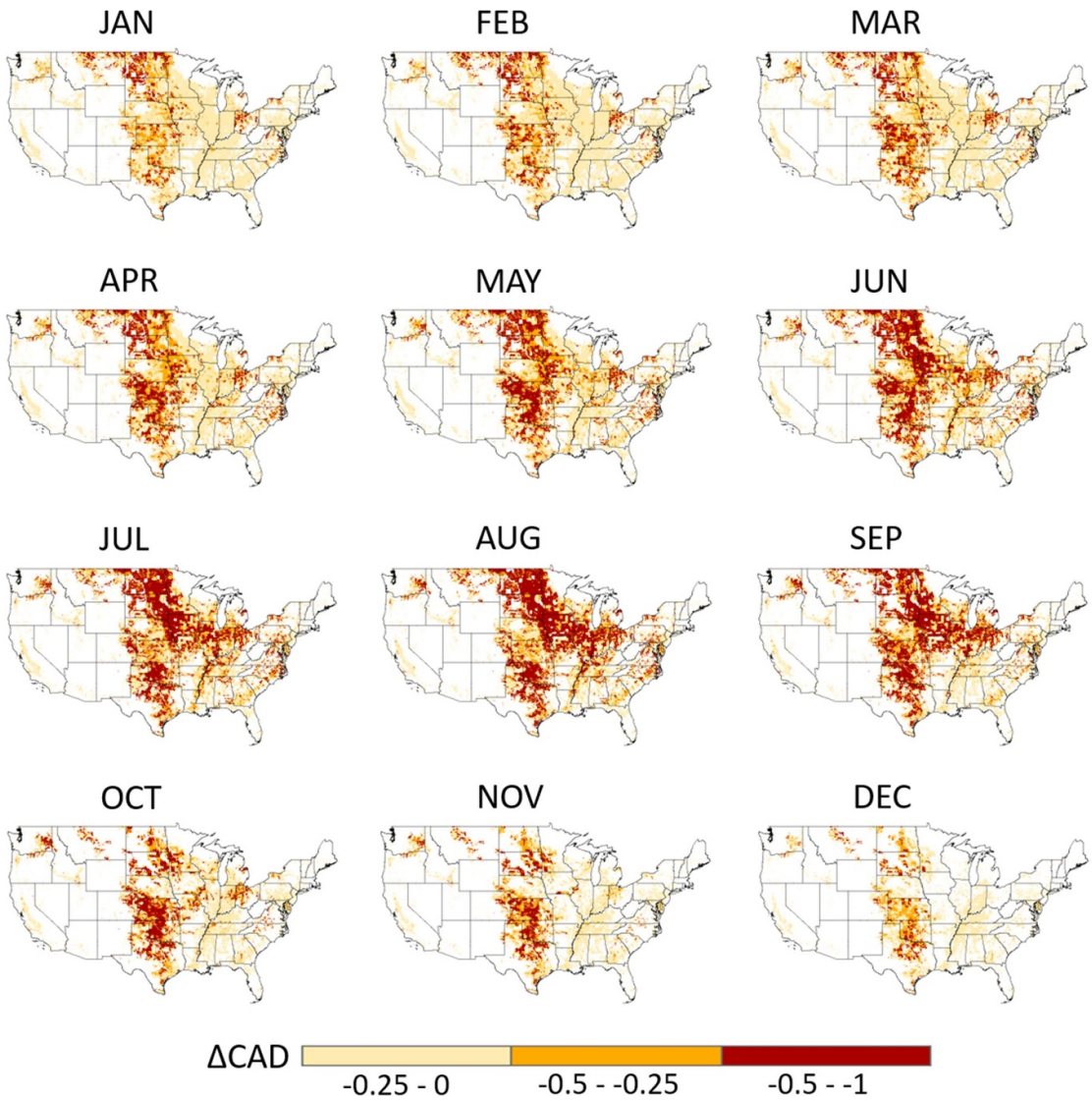

Figure 1. Spatial distribution of the difference in CAD (ΔCAD) after and before the RFtoIF transition. Negative values indicate a decrease in CAD (or an increase in blue water scarcity) with RFtoIF transition.

The impact can be gauged both in terms of intensification and spatial proliferation of blue water scarcity. Around 5.3 million hectares (27.2 million hectares) of land that did not undergo RFtoIF transition in S2 face spatial proliferation (intensification) in blue water scarcity (figure S5).

3.2. RFtoIF transition and the urban water security

RFtoIF transition, which is primarily concentrated in rural areas (see definition in rural areas in 2.1) with 97% of the RFtoIF transitioned land lying within it, may have significant impacts on the urban water security. Analyses of blue water scarcity over LUCs (see *Methods: Water Supply Data of LUCs*) for which detailed data of water supply infrastructure is publicly available, show evidence of both spatial proliferation and intensification of blue water scarcity in them. CAD estimates over LUCs are evaluated to assess the differential impacts of RFtoIF transition on them. The impact of RFtoIF transition is significant in LUCs, with spatial proliferation (intensification) of blue water scarcity increasing by 0.97 million hectares (8.2 million hectares), i.e. around 4.4% (37.5%) of the total area of LUCs considered in this study. Before RFtoIF transition, i.e. in scenario S1, 86.2% of LUC and 90.2% of rest of the area (henceforth referred to as ROA) model cells have CAD values greater than 0.8, which belongs to a low or no water scarcity category (figure 2). After the RFtoIF transition, the percent of cells that face no or low water scarcity reduces to 84.3% and 67.8% for LUCs and ROA, respectively. In contrast, 13% of the total ROA cells are estimated to face a moderate blue water scarcity after the transition, while it was 5.3% in S1. The LUCs also see a hike in the number of cells facing moderate blue water scarcity after transition with fractional area rising to 9.2% from 7.8%.

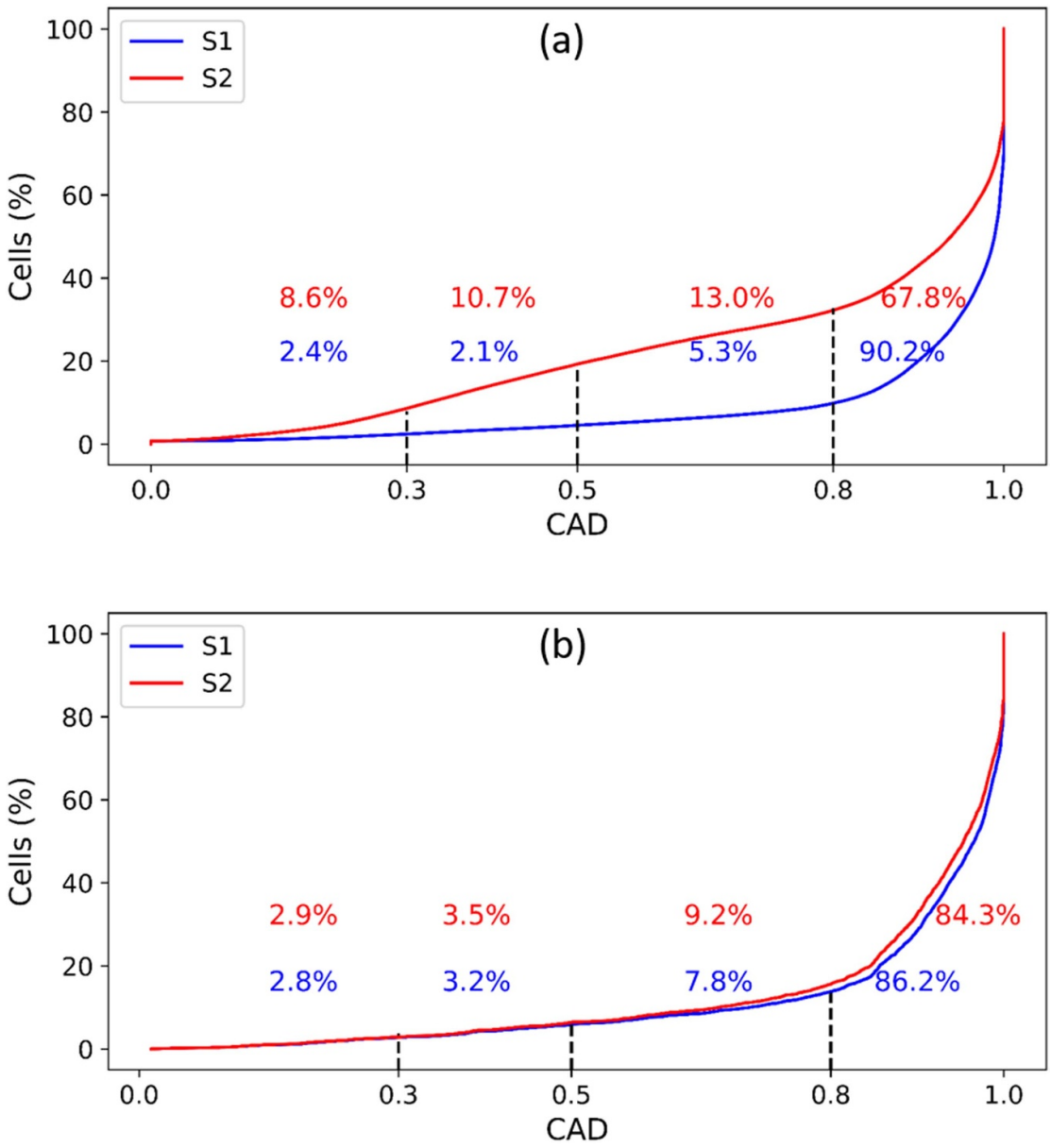

Figure 2. Cumulative distribution function of CAD values for ROA (a), and LUC cells (b) for scenarios S1 (blue) and S2 (red). The numbers indicate the percent of cells belonging to different blue water scarcity classes i.e. low ($0.8 < \text{CAD} \leqslant 0.99$), moderate ($0.5 < \text{CAD} \leqslant 0.8$), high ($0.3 < \text{CAD} \leqslant 0.5$), or severe ($\text{CAD} \leqslant 0.3$). Fraction of the cells with low or no water scarcity reduces after the RFtoIF transition in both LUCs and ROA. The reduction in fraction of ROC cells is relatively larger.

Results show that 24 (18) out of 53 highly populated LUCs face a blue water scarcity with at least a moderate intensity for a minimum of one month (six months), respectively (figure 3) before RFtoIF transition. These 24 urban areas have a population of around 82 million and roughly constitute 25% of the total US population. The number rises to 29 cities facing blue water scarcity for at least one month with a population of around 97 million urban population or 29.5% of the US population after the RFtoIF transition. In addition, urban agglomerations of Columbus in OH, Dallas–Fort Worth–Arlington in TX, Houston in TX, Memphis in TN—MS—AR, Minneapolis–St. Paul in MN—WI, and Virginia Beach in VA face moderate water scarcity ($0.5 < \text{CAD} \leqslant 0.8$) for at least one extra month after RFtoIF transition. Overall, RFtoIF transition increases scarcity in 6 out of 53 urban areas, affecting additional 16 million people. Notably, none of the six LUCs facing an increase in scarcity with RFtoIF transition are located in arid regions, as their upstream regions already have a high irrigation fraction, and hence the changes in abstraction with RFtoIF transition is small.

3.3. Variables that influence the spatial distribution and intensity of blue water scarcity, and changes in it due to RFtoIF transition

The spatial distribution of CAD is found to be largely controlled by the relative availability of water from

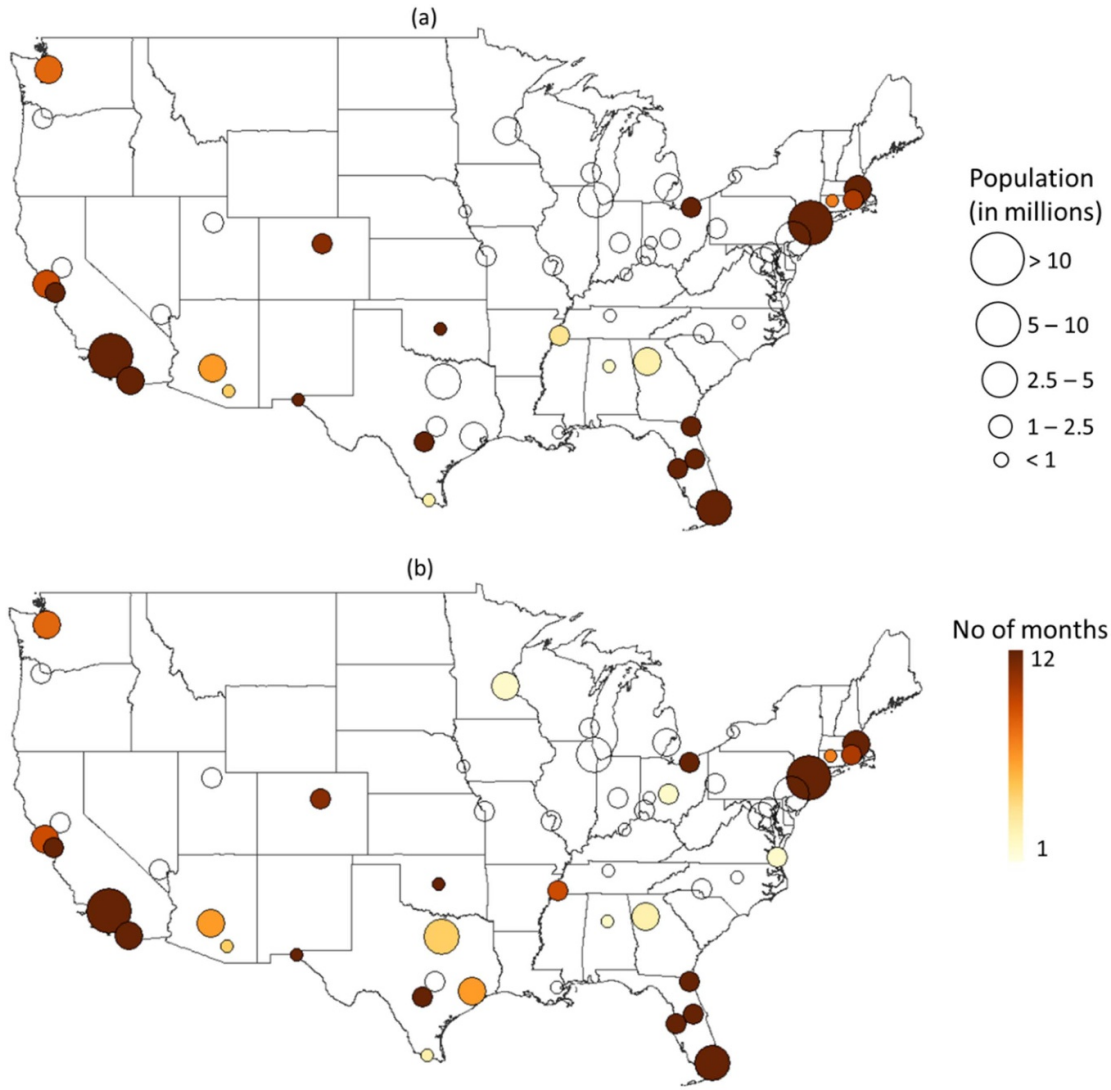

Figure 3. Blue water scarcity for 53 LUCs for scenarios S1 (a) and S2 (b). The size of the circle represents the population, and the color represents the number of months a LUC faces water scarcity.

upstream. Locations (or model cells) receiving high incoming lateral flow, which refers to locally generated runoff and water transferred through canals from adjacent cells, or runoff generally have higher CAD values or low blue water scarcity (figure 4(a)). For example, among cells with CAD $\leqslant$ 0.5, around 55% of them have a lateral flow of less than 0.0001 MCM per day. For non-urban cells, CAD distribution is affected by crop area as well, as water demand increases with higher crop area. Grids in Midwestern US and Central Valley region have higher crop area and hence often have low CAD values. Despite having higher lateral flow, many grids experience lower CAD values due to high crop fraction (figure 4(a)). Further analysis shows a large number of such grids are situated in the dense cropped regions of Midwestern US and lower Missouri river basin. In contrast, for LUC cells that usually do not have any significant fraction of croplands, the water demand and consequently the CAD is influenced by the human population. Cells with less population and large lateral flow tend to show higher CAD values or less blue water scarcity (figure 4(b)). Cells with high population and low lateral flow but still higher CAD are the regions that receive water from distant withdrawal points.

The change in blue water scarcity is quantified by ΔCAD, which is either zero or negative. Of the LUC cells that experience a change in CAD, most observe ΔCAD between 0 to -0.2 (table S3 and figure S6). The same is true for non-transitioned ROA cells. Among the ROA cells that undergo transition, a large fraction of them (>70%) have ΔCAD <-0.2. Around 5.7% of the transitioned grids have ΔCAD ranging from -1 to -0.8. Overall, when all cells are considered, more than 24% of the cells experience ΔCAD <-0.2.

To understand the influences on the spatial distribution of ΔCAD, ΔCAD for LUC and ROA cells are expressed as:

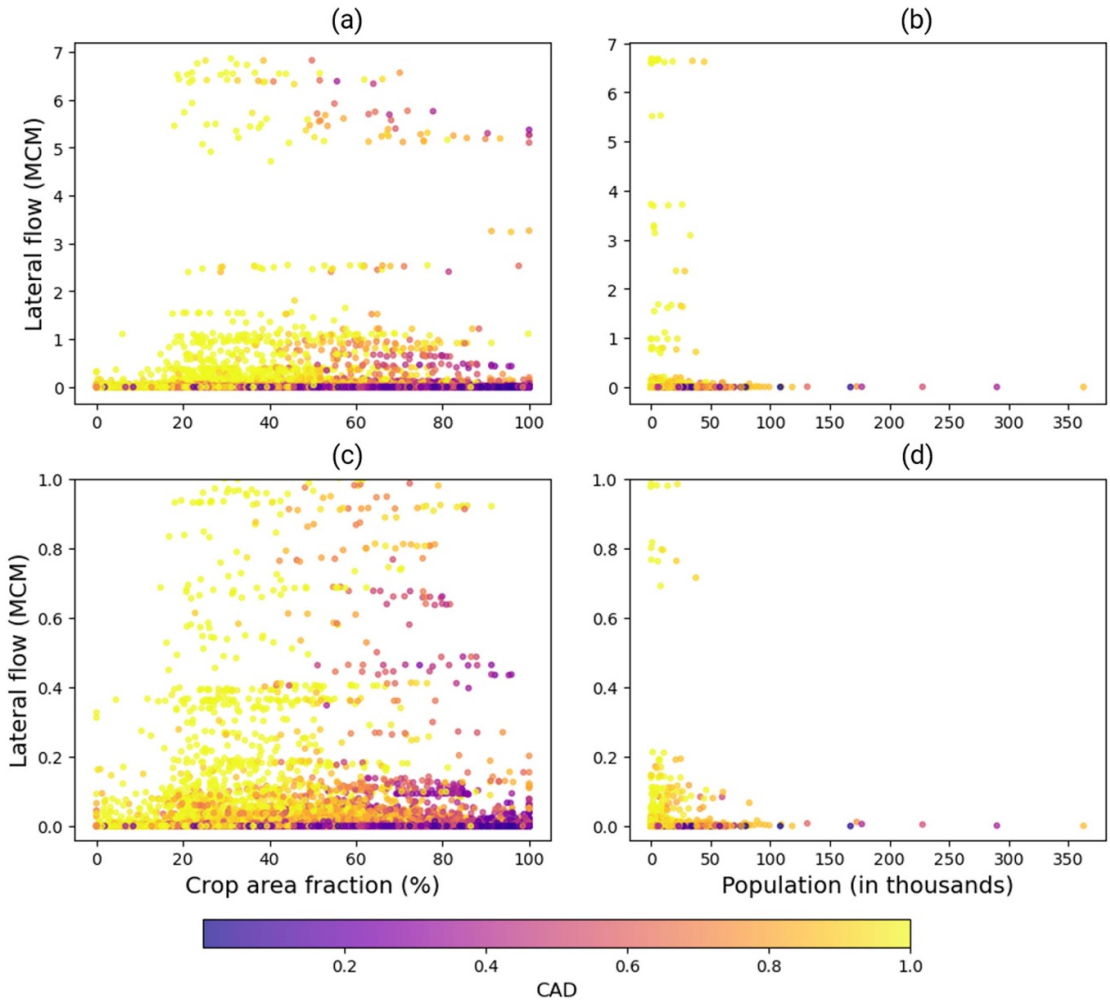

Figure 4. (a) CAD for ROA cells as a function of their lateral flow input and crop area percentage. Cells with high crop area and low lateral flow have lower CAD values. (b) CAD for LUC cells vis-à-vis lateral flow and population. (c) and (d) are same as (a) and (b), respectively, but zoomed-in for low lateral flow values. The figure illustrates the interplay of factors controlling water demand (e.g. crop area fraction and population) and supply (lateral flow input) in agriculture and urban settings.

$$\Delta CAD = \frac{A2}{D2} - \frac{A1}{D1} = \frac{A2 - A1}{D2} - \frac{A1}{D2.D1}(D2 - D1) = \frac{(A2 - A1) - \frac{A1}{D1}(D2 - D1)}{D2} \quad (3)$$

$$\rightarrow \Delta\text{CAD} = \frac{\Delta\text{abs} - \frac{A1}{D1} * \Delta\text{dem}}{D1 + \Delta\text{dem}} \quad (4)$$

where, $A1$ and $D1$ ($A2$ and $D2$) are the water abstraction and demand in scenario S1 (S2), respectively. Δabs (=$A2$–$A1$) and Δdem (=$D2$–$D1$) represent the change in water abstraction and demand due to transition, respectively. Δdem is either zero or positive while Δabs is either negative or positive depending on the availability of excess water available for abstraction following RFtoIF transition.

For LUCs, since the water demand remains the same in both scenarios because of the absence of RFtoIF transition in them, Δdem is zero and the equation (4) reduces to:

$$\Delta\text{CAD} = \frac{\Delta\text{abs}}{D1}. \quad (5)$$

As indicated in equation (5), ΔCAD increases as the magnitude of Δabs increases for LUC cells (figure 5(a)). For a given Δabs, high-demand LUCs that are primarily the areas with high population density or industrialization experience smaller change in CAD or blue water scarcity. Conversely, ΔCAD is generally higher for urban areas which experience a higher reduction in water abstraction (figure S7). LUCs with higher Δabs experience a reduction in CAD value after the transition. For example, Houston, TX receives water from Lake Livingston on the Trinity River, and Lake Houston and Lake Conroe on the San Jacinto River, for its daily domestic and industrial needs and does not face water scarcity in S1. After irrigation expansion in scenario S2, predicted water availability in current surface water sources reduces and the existing water transport infrastructure is unable to meet the city water demands. Thus, the number of water-scarce

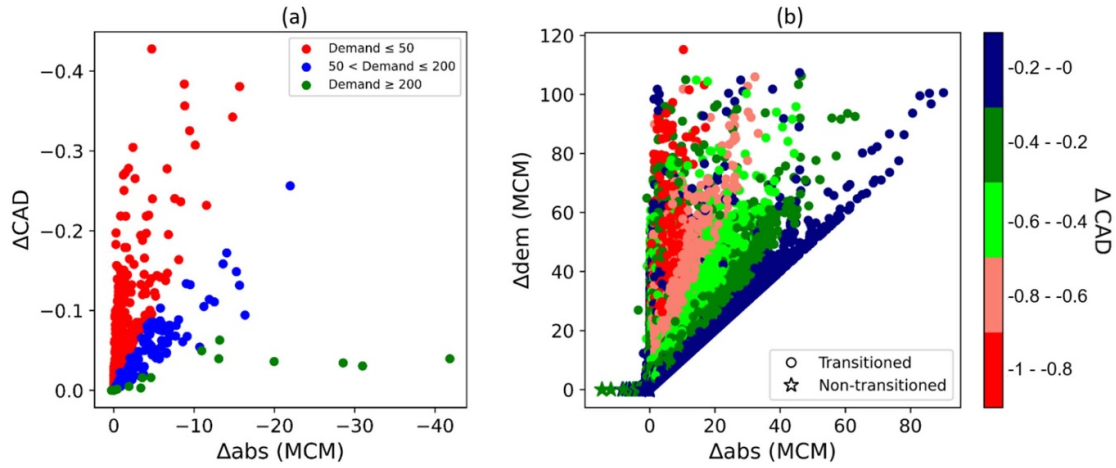

Figure 5. (a) Scatter plot between annual average ΔCAD and Δabs for LUC cells. Cells with higher demand (shown in million cubic meter per year (MCM/year)) have smaller ΔCAD for the same Δabs, (b) annual average Δabs and Δdem scatter plot for ROA cells. Some of the non-transitioned cells show change in CAD even after no change in demand in scenario S2. For transitioned grids, change in CAD is higher for the cells with less increase in abstraction i.e. low Δabs, while cells with high Δabs have less change in CAD.

months rises to 6 in S2. The largest reduction in water abstraction is observed in September, when it reduces by around 10%. The mean annual water abstraction reduces by around 4%. Consequently, CAD reduces for all the months. Blue water scarcity changes from no or low to moderate for May–October. A similar picture unfolds in Dallas, where water scarcity months rise from 0 to 4 due to reduced water availability in the city's water resources. Along similar lines, Columbus, OH; Memphis, TN—MS—AR; Minneapolis–St. Paul, MN—WI; and Virginia Beach, VA have large absolute Δabs and face at least one additional month of water scarcity. Notably, urban agglomerations with sufficient excess water supply and/or minimal RFtoIF transition upstream manage to be unaffected by RFtoIF transition. For example, two major urban agglomerations in Arizona, viz. Phoenix-Mesa and Tucson experience blue water scarcity for 6 and 4 months, respectively, in both scenarios S1 and S2, as relatively small increase in water withdrawal from RFtoIF transition can be supplemented by water supply from Central Arizona Project reservoirs (Tucson and Phoenix-Mesa) and Salt Lake Project (Phoenix-Mesa). In a few circumstances, number of months experiencing changes in scarcity may be zero because they may already be scarce in all months in scenario S1. For example, New York—Newark, Oklahoma City, and San Antonio, already experience a full year of water scarcity, indicating that no further months are added in those cities. It is to be noted that for several LUCs, such as Milwaukee, Kansas City, Chicago, and St. Louis, while RFtoIF transition in the upstream contribution area decreased river flow causing negative change in abstraction from it (figure 6), local water sources in the neighborhood that supply water through canals are able to cushion this reduction (as indicated by positive change in abstraction from canals). In contrast, LUCs that experience increase in number of months of scarcity generally experience negative change in abstraction from both rivers and the canals. This highlights that the impact of RFtoIF transition on scarcity can be mediated by ancillary water sources that are not directly or significantly impacted by RFtoIF transition.

For ROA cells, in addition to Δabs and $D1$, the spatial distribution of ΔCAD is controlled by additional variables including Δdem and $A1$ (see equation (4)). Notably, among the ROAs, most transitioned locations have positive Δabs, while the non-transitioned cells either have zero or negative Δabs (figure 5(b)). This suggests that transitioned cells withdraw more water to match the demand after RFtoIF transition, while cells that do not participate in transition withdraw less or the same amount of water depending on the extent of reduction in water availability at the location. ΔCAD for non-transitioned ROA cells behaves like that of LUC cells, with its absolute value increasing with an increase in Δabs. In contrast, at the transitioned ROA locations, the absolute value of ΔCAD decreases with an increase in Δabs magnitude for a given Δdem. In other words, if the increase in abstraction does not match the increase in water demand, transitioned locations experience higher ΔCAD. To conclude, figure 5 shows the characteristics of the urban and rural cells based on their change in demand, abstraction and CAD after RFtoIF transition. It captures the intricate interplay of water demand and availability factors that shape water scarcity under land use change. The analysis identifies cells prone to heightened scarcity from irrigation expansion, aiding targeted sustainable management.

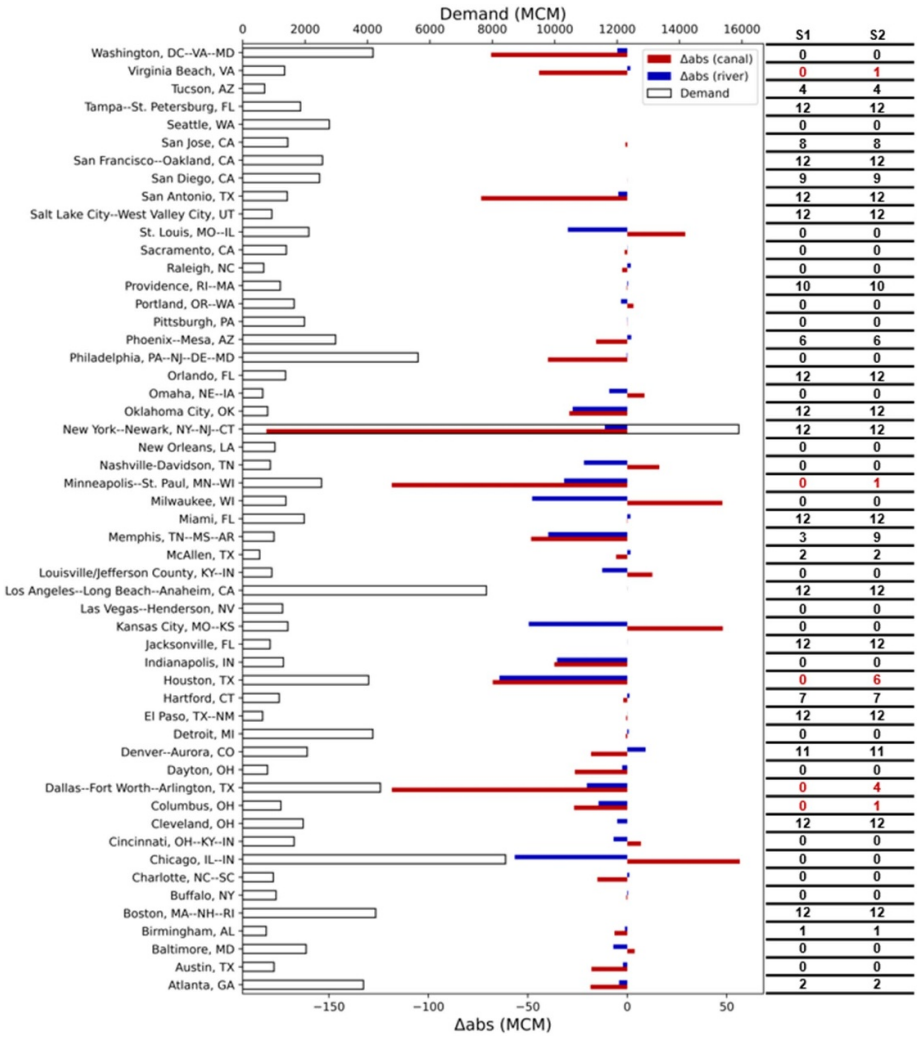

Figure 6. 53 LUCs considered in this study and their average annual water demand and Δabs. The Δabs is specified separately based on the source of water abstraction i.e. river and canal. Water abstraction from water withdrawal points is included in canal water abstraction. Column on the right indicates number of months of water scarcity in scenarios S1 and S2 for each considered LUC.

4. Discussion and synthesis

It is well known that transitioning from rainfed to irrigation-fed agriculture boosts crop yields and improves food security. Our continental hydrologic simulation, however, shows that RFtoIF transition over croplands that experience green water scarcity for an average of at least one month a year intensifies freshwater scarcity in both transitioned and non-transitioned areas. Notably, increase in scarcity in urban areas is not dominated by those situated in arid settings. Instead, it depends on a multitude of factors ranging from increase in water abstraction in the upstream, magnitude of water demand in the urban region, and buffer amount available in nearby water withdrawal points. Our simulation results show that among just the 53 considered LUCs, around 16 million additional urban residents will get affected by such a transition. This may increase the risk of water conflict between urban and the surrounding upstream rural water users, as it is being realized in many water stressed situations throughout the world [55–59]. Notably, large urban areas with improved water infrastructure are better equipped to meet the increased water demand resulting from additional water usage for irrigation, mitigating the impact of water scarcity in these regions. The analysis was conducted assuming all rainfed areas facing green water scarcity for at least one month are converted to irrigation fed, which while being an unlikely scenario in terms of its implementation, helps highlight the degree of impact that may be incurred. Additional sensitivity analysis to assess the impact of GWS threshold and number of months on the total green water scarce area shows that the total area facing green water scarcity does not change much for low GWS threshold values (GWS $<= 0.3$) or the number of minimum number of months ($<= 3$) considered (figure S8). Ideally, identification of GWS threshold or related drivers that trigger RFtoIF transition or determine the extent of RFtoIF intensification would allow for a more realistic RFtoIF transition scenario.

However, such a determination remains challenging due to the influence of a range of factors including economic conditions of farmers, incentives provided by local/federal government, penetration of agricultural extension education among the farming community, farmers' social networks, water availability, political considerations, water use by other sectors, water infrastructure, and more [43, 60–64]. The study does not account for water consumption by poultry and livestock in agricultural sectors. The impact of RFtoIF transition on the increase in the number of livestock and consequently water use by them [65] is also not considered here. A model facilitating livestock and other farm water consumption may be used to assess the overall impact. However, the water use by livestock is minimal as compared to other sectors (less than 1% of total freshwater withdrawals in 2000) [66].

The water scarcity evaluations performed here are based on the historical datasets, i.e. crop area distribution and irrigated area maps circa 2000 and 2005, respectively. Given that new and better data is continuously being generated, the reported population facing blue water scarcity in the status quo and transition scenario are expected to change with their usage. It is also to be noted that by the year the full RFtoIF transition (as simulated in S2) may get realized, if it ever does, the climate is likely to be different. However, given the uncertainty in timeline of this transition, the current study does not consider the concomitant impacts of changes in climate on evapotranspiration, precipitation, water availability, and water demand [67, 68]. During the transition, other socioeconomic changes such as urban and rural demographics, water infrastructure technology, economic changes, changes in water withdrawal efficiency for all three sectors, cropping patterns, agricultural management practices, land cover change, etc. are subject to change and may affect the water scarcity in an area as well. These factors are not explicitly considered in the scenario simulations performed here. We further acknowledge that the RFtoIF transition may disturb local hydrological cycle and affect the precipitation, evapotranspiration, surface temperature, and other land atmospheric interactions [69–71]. These factors can affect the water scarcity estimates as well.

It is to be noted that just as is the case with most model implementations, the H08 model results, which have been used to obtain the scenario simulations in this study, suffer from model structure and data uncertainty. For example, as the model does not consider lateral groundwater flow between cells, it may have impacted the estimates of the spatial distribution of CAD and ΔCAD as groundwater withdrawals may directly impact the surface water resources [72, 73]. Uncertainties also exist in terms of accounting for all the possible surface water supplies. An effort has been made in this study to reduce this uncertainty by including urban water withdrawal points [39]. A more accurate dataset on distant water supply may improve the results. Notably, only surface urban withdrawal points were considered, due to their ability to be incorporated as canal origin points in the current version of H08. This may result in an overestimation of blue water scarcity in cities that rely primarily on groundwater or desalinization for their municipal and industrial water demand. Another source of uncertainty may arise due to the current representation of urban water withdrawal points in H08. Specifically, while all LUC grids are able to abstract water from urban withdrawal points, the grids that come first in the pre-defined sequence are prioritized for withdrawal. This could potentially impact water scarcity at the grid scale, although the overall effect on the LUC level is likely to be minimal as the abstraction from all grids is aggregated to calculate the total water abstracted by the LUCs. Furthermore, the study assumes that the domestic sector is the first to extract water, followed by the industrial and then the agricultural sectors. Assuming agriculture has the lowest priority in water abstraction is a pragmatic choice given the lack of information on which regions prioritize which sectors. However, the results of water scarcity can be sensitive to this assumption. According to Flörke *et al* [38], climate change affects the surface water deficit in urban areas in significantly different ways depending on the water extraction priority assigned to the urban population. Here, we performed an additional analysis by assigning agriculture as the first priority and the domestic sector as the last for water abstraction. The altered hierarchy in water use resulted in increase in water scarcity in 7 LUCs in S2 (previously, the increase was noted in 6 LUCs). Notably, the average change in CAD in urban areas after RFtoIF transition for this new water abstraction priority configuration rose by around 30%, indicating more urban grids with water scarcity. These results highlight that establishing appropriate water withdrawal priorities in river basins can help mitigate RFtoIF transition's impact.

In this study, areas facing water scarcity are derived using the CAD index. The index is similar to other commonly employed water scarcity indices such as the criticality ratio [74], Falkenmark index [29], and water footprint based index [75–77]. Previous studies [24, 45] have shown that estimates of population experiencing scarcity are only mildly sensitive to the choice of water scarcity metrics (table S1(a)), and there is a close correspondence between these indices. This is unsurprising as majority of these metrics use two similar primary variables, namely the abstracted water amount or the water available for abstraction, and demand or water footprint (table S1(b)). Differences between metrics may arise from the inclusion of additional variables, such as accounting of water-use losses in water abstraction term or the numerator of CAD. The magnitude of

these additional variables can lead to variations in the estimates of water scarcity across metrics. It is worth noting that each metric often applies subjective thresholds to classify the severity of scarcity, which can also contribute to disparities in results between metrics.

Apart from these, uncertainties may also occur due to the use of spatially uniform irrigation and, domestic and industrial water use efficiencies, which are set to 0.6, 0.15, and 0.1, respectively, over all the cells. Furthermore, the results are based on a temporally static distribution of irrigation area, cropland-pasture fraction, and areas of different crops over the simulation period. The industrial and domestic water withdrawal used in this study is obtained from AQUASTAT and downscaled to the modeling scale of 5 × 5 arcmin based on the population distribution. Notably, the temporal variation of domestic and industrial water withdrawal is also not taken into consideration. This issue can be attenuated if the model is supplied with more accurate data on water withdrawal by domestic and industrial sectors. CAD and ΔCAD estimates are likely to be also affected by uncertainties in EFR, which here is defined based on the monthly average river discharge [52]. Studies [78] have previously reported that the EFR estimation method may determine water scarcity assessment, although Mekonnen and Hoekstra [28] also noted that the population living under moderate blue water scarcity does not change significantly for the uncertainty range of EFR. Another source of uncertainty is from the current AET and PET parameterizations, which do not account for crop-specific stomatal conductances. Given that these conductances may vary with crops and cultivars [79], uncertainties in PET and ET estimates can be reduced by performing calibration and validation against remotely-sensed evapotranspiration estimates [80].

Despite the aforementioned methodological limitations, the analysis clearly shows that the controls on changes in blue water scarcity (or ΔCAD) are different between non-transitioned and transitioned locations. The trend of changes in ΔCAD vis-à-vis changes in abstraction is also contrasting between non-transitioned and transitioned locations. In addition, the effects of RFtoIF transition on urban areas, especially in regards to additional months being affected by scarcity is dependent both on antecedent scarcity state before transition and presence of ancillary water supply sources to cities either from reservoirs or locations that are not directly impacted by RFtoIF transition. Overall, the results indicate that upstream of urban areas with low irrigation expansion (e.g. LUCs like Los Angeles—Long Beach—Anaheim, CA; Las Vegas—Henderson, NV; Birmingham, AL; Atlanta, GA; Salt Lake City—West Valley City, UT; Hartford, CT; and Raleigh, NC) or those equipped with more robust water infrastructure with ample buffer supply sources (e.g., cities like St. Louis, MO—IL; Cincinnati, OH—KY—IN; Phoenix—Mesa, AZ; etc.), may be more suitable for undergoing a transition to irrigated agriculture (figure S9). It is to be noted that just because some LUCs experience a large change in ΔCAD doesn't necessarily imply that transitions in the neighboring ROA are unlikely. Factors such as political support, economic soundness of LUCs, the significance of water for both LUC and ROA users, impacts on water quality, and other considerations may ultimately determine the feasibility and support for RFtoIF transition. Future studies may perform an integrated wholistic assessment of all the drivers, stresses, impacts and responses at each LUCs to help identify cities that can best adapt to unsustainable irrigation expansion.

Overall, the study indicates that the irrigation expansion, if not properly managed, is unsustainable. Furthermore, irrigation expansion can enhance water scarcity in large urban areas and could be a conflict agent between urban and rural water users. Given the existing significant divide in the urban-rural electorate in US [81], these conflicts are likely to get aggravated and spur social and administrative challenges regarding water allocation and access. Alterations in water resources due to rapid urbanization, and socio-economic and climate change, are likely to further pose challenges for water managers [82–87]. Since the impacts of RFtoIF transition propagate downstream, constraining urban-rural conflicts [55–59] may require update and/or formulation of innovative basin-scale water apportioning doctrines and compacts. Alternative solutions to mitigate these negative impacts include changing cropping pattern and practices [17, 88, 89], and enhancing the sustainability of virtual water trade [90–92].

Data availability statement

The data that support the findings of this study are openly available at the following URL/DOI: https://zenodo.org/record/7641692.

Acknowledgments

M K acknowledges support from the National Science Foundation (NSF, Grant Nos. EAR-1856054 and OIA-2019561).

Author contributions

M K conceived the study, acquired funding, and provided project administration and supervision. L R compiled the data, performed model simulations, developed relevant codes for analyses and visualizations, and generated model outputs. L R and M K designed the methodology, performed data analyses,

and drafted the manuscript. N H and P R contributed to model implementation. All authors edited the manuscript and helped improve it.

Conflict of interest

The authors declare no competing interests.

Open research

Data analyses were performed using Python (version 3.8), major libraries used are: pandas, numpy, scipy, os, glob, arcpy, geopandas, and matplotlib. The datasets generated and/or analysed during the current study are available in the Zenodo repository (see link: https://zenodo.org/record/7641692).

ORCID iDs

Lokendra S Rathore https://orcid.org/0000-0001-7024-2361
Mukesh Kumar https://orcid.org/0000-0001-7114-9978
Naota Hanasaki https://orcid.org/0000-0002-5092-7563
Pushpendra Raghav https://orcid.org/0000-0002-2982-069X

References

[1] Godfray H C J, Beddington J R, Crute I R, Haddad L, Lawrence D, Muir J F, Pretty J, Robinson S, Thomas S M and Toulmin C 2010 Food security: the challenge of feeding 9 billion people *Science* **327** 812–8
[2] Tilman D, Balzer C, Hill J and Befort B L 2011 Global food demand and the sustainable intensification of agriculture *Proc. Natl Acad. Sci.* **108** 20260–4
[3] Beltran-Peña A, Rosa L and D'Odorico P 2020 Global food self-sufficiency in the 21st century under sustainable intensification of agriculture *Environ. Res. Lett.* **15** 095004
[4] Foley J A *et al* 2011 Solutions for a cultivated planet *Nature* **478** 337–42
[5] Cirera X and Masset E 2010 Income distribution trends and future food demand *Phil. Trans. R. Soc.* B **365** 2821–34
[6] Garnett T *et al* 2013 Sustainable intensification in agriculture: premises and policies *Science* **341** 33–34
[7] Davis K F, Gephart J A, Emery K A, Leach A M, Galloway J N and D'Odorico P 2016 Meeting future food demand with current agricultural resources *Glob. Environ. Change* **39** 125–32
[8] Davis K F, Downs S and Gephart J A 2021 Towards food supply chain resilience to environmental shocks *Nat. Food* **2** 54–65
[9] Ray D K, West P C, Clark M, Gerber J S, Prishchepov A V, Chatterjee S and Jung Y H 2019 Climate change has likely already affected global food production *PLoS One* **14** e0217148
[10] Richards R A, Rebetzke G J, Condon A G and van Herwaarden A F 2002 Breeding opportunities for increasing the efficiency of water use and crop yield in temperate cereals *Crop Sci.* **42** 111–21
[11] Raines C A 2011 Increasing photosynthetic carbon assimilation in C3 plants to improve crop yield: current and future strategies *Plant Physiol.* **155** 36–42
[12] Smith R G, Gross K L and Robertson G P 2008 Effects of crop diversity on agroecosystem function: crop yield response *Ecosystems* **11** 355–66
[13] Wang Y, Xie Z, Malhi S S, Vera C L, Zhang Y and Wang J 2009 Effects of rainfall harvesting and mulching technologies on water use efficiency and crop yield in the semi-arid Loess Plateau, China *Agric. Water Manage.* **96** 374–82
[14] Blum A 2009 Effective use of water (EUW) and not water-use efficiency (WUE) is the target of crop yield improvement under drought stress *Field Crops Res.* **112** 119–23
[15] Su Z, Zhang J, Wu W, Cai D, Lv J, Jiang G, Huang J, Gao J, Hartmann R and Gabriels D 2007 Effects of conservation tillage practices on winter wheat water-use efficiency and crop yield on the Loess Plateau, China *Agric. Water Manage.* **87** 307–14
[16] Rising J and Devineni N 2020 Crop switching reduces agricultural losses from climate change in the United States by half under RCP 8.5 *Nat. Commun.* **11** 4991
[17] Xie W, Zhu A, Ali T, Zhang Z, Chen X, Wu F, Huang J and Davis K F 2023 Crop switching can enhance environmental sustainability and farmer incomes in China *Nature* **616** 300–5
[18] Rosa L, Rulli M C, Davis K F, Chiarelli D D, Passera C and D'Odorico P 2018 Closing the yield gap while ensuring water sustainability *Environ. Res. Lett.* **13** 104002
[19] Rosa L, Chiarelli D D, Sangiorgio M, Beltran-Peña A A, Rulli M C, D'Odorico P and Fung I 2020 Potential for sustainable irrigation expansion in a 3 °C warmer climate *Proc. Natl Acad. Sci.* **117** 29526–34
[20] Tuninetti M, Ridolfi L and Laio F 2020 Ever-increasing agricultural land and water productivity: a global multi-crop analysis *Environ. Res. Lett.* **15** 0940a2
[21] Troy T J, Kipgen C and Pal I 2015 The impact of climate extremes and irrigation on US crop yields *Environ. Res. Lett.* **10** 054013
[22] Zaveri E and Lobell D B 2019 The role of irrigation in changing wheat yields and heat sensitivity in India *Nat. Commun.* **10** 4144
[23] Alexandratos N World Agriculture towards 2030/2050: the 2012 revision.:154
[24] Hanasaki N, Kanae S, Oki T, Masuda K, Motoya K, Shirakawa N, Shen Y and Tanaka K 2008 An integrated model for the assessment of global water resources—part 2: applications and assessments *Hydrol. Earth Syst. Sci.* **12** 1027–37
[25] Qi X, Feng K, Sun L, Zhao D, Huang X, Zhang D, Liu Z and Baiocchi G 2022 Rising agricultural water scarcity in China is driven by expansion of irrigated cropland in water scarce regions *One Earth* **5** 1139–52
[26] McDermid S S, Mahmood R, Hayes M J, Bell J E and Lieberman Z 2021 Minimizing trade-offs for sustainable irrigation *Nat. Geosci.* **14** 706–9
[27] Samimi M, Mirchi A, Moriasi D, Sheng Z, Gutzler D, Taghvaeian S, Alian S, Wagner K and Hargrove W 2023 Adapting irrigated agriculture in the middle Rio Grande to a warm-dry future *J. Hydrol. Reg. Stud.* **45** 101307
[28] Mekonnen M M and Hoekstra A Y 2016 Four billion people facing severe water scarcity *Sci. Adv.* **2** e1500323
[29] Falkenmark M 1989 The massive water scarcity now threatening Africa: why isn't it being addressed? *Ambio* **18** 112–8
[30] Falkenmark M, Lundqvist J and Widstrand C 1989 Macro-scale water scarcity requires micro-scale approaches *Nat. Resour. Forum* **13** 258–67
[31] Oki T and Kanae S 2006 Global hydrological cycles and world water resources *Science* **313** 1068–72
[32] Vöörösmarty C J, Green P, Salisbury J and Lammers R B 2000 Global water resources: vulnerability from climate change and population growth *Science* **289** 284–8
[33] Alcamo J and Henrichs T 2002 Critical regions: a model-based estimation of world water resources sensitive to global changes *Aquat. Sci.* **64** 352–62

[34] Wada Y, Van Beek L P H, Viviroli D, Dürr H H, Weingartner R and Bierkens M F P 2011 Global monthly water stress: 2. Water demand and severity of water stress *Water Resour. Res.* **47** W07518
[35] Hoekstra A Y, Mekonnen M M, Chapagain A K, Mathews R E and Richter B D 2012 Global monthly water scarcity: blue water footprints versus blue water availability *PLoS One* **7** e32688
[36] Liu X, Liu W, Tang Q, Liu B, Wada Y and Yang H 2022 Global agricultural water scarcity assessment incorporating blue and green water availability under future climate change *Earth's Future* **10** e2021EF002567
[37] He C, Liu Z, Wu J, Pan X, Fang Z, Li J and Bryan B A 2021 Future global urban water scarcity and potential solutions *Nat. Commun.* **12** 4667
[38] Flörke M, Schneider C and McDonald R I 2018 Water competition between cities and agriculture driven by climate change and urban growth *Nat. Sustain.* **1** 51–58
[39] McDonald R I *et al* 2014 Water on an urban planet: urbanization and the reach of urban water infrastructure *Glob. Environ. Change* **27** 96–105
[40] Walton B 2019 U.S. irrigation continues steady eastward expansion *Circle of Blue* (available at: www.circleofblue.org/2019/world/u-s-irrigation-continues-steady-eastward-expansion/) (Accessed 19 December 2022)
[41] Bureau U C TIGER/line shapefiles (The United States Census Bureau) (available at: www.census.gov/geographies/mapping-files/time-series/geo/tiger-line-file.html) (Accessed 19 June 2021)
[42] Center For International Earth Science Information Network-CIESIN-Columbia University 2018 Gridded population of the world, version 4 (GPWv4): population count, revision 11 (NASA Socioeconomic Data and Applications Center (SEDAC)) (available at: https://sedac.ciesin.columbia.edu/data/set/gpw-v4-population-count-rev11) (Accessed 21 April 2022)
[43] Rosa L, Chiarelli D D, Rulli M C, Dell'Angelo J and D'Odorico P 2020 Global agricultural economic water scarcity *Sci. Adv.* **6** eaaz6031
[44] Hanasaki N, Kanae S, Oki T, Masuda K, Motoya K, Shirakawa N, Shen Y and Tanaka K 2008 An integrated model for the assessment of global water resources—part 1: model description and input meteorological forcing *Hydrol. Earth Syst. Sci.* **12** 1007–25
[45] Hanasaki N, Yoshikawa S, Pokhrel Y and Kanae S 2018 A quantitative investigation of the thresholds for two conventional water scarcity indicators using a state-of-the-art global hydrological model with human activities *Water Resour. Res.* **54** 8279–94
[46] Monfreda C, Ramankutty N and Foley J A 2008 Farming the planet: 2. Geographic distribution of crop areas, yields, physiological types, and net primary production in the year 2000 *Glob. Biogeochem. Cycles* **22** GB1022
[47] Siebert S, Kummu M, Porkka M, Döll P, Ramankutty N and Scanlon B R 2015 A global data set of the extent of irrigated land from 1900 to 2005 *Hydrol. Earth Syst. Sci.* **19** 1521–45
[48] Xia Y, Mitchell K, Ek M, Sheffield J, Cosgrove B and Wood E 2012 Continental-scale water and energy flux analysis and validation for the North American land data assimilation system project phase 2 (NLDAS-2): 1. Intercomparison and application of model products *J. Geophys. Res. Atmos.* **117** D03109
[49] Ramankutty N, Evan A T, Monfreda C and Foley J A 2008 Farming the planet: 1. Geographic distribution of global agricultural lands in the year 2000 *Glob. Biogeochem. Cycles* **22** GB1003
[50] Food and Agriculture Organization (FAO) AQUASTAT database (available at: www.fao.org/aquastat/statistics/query/index.html) (Accessed 19 June 2021)
[51] Hanasaki N, Yoshikawa S, Pokhrel Y and Kanae S 2018 A global hydrological simulation to specify the sources of water used by humans *Hydrol. Earth Syst. Sci.* **22** 789–817
[52] Shirakawa N 2005 Global estimation of environmental flow requirement based on river runoff seasonality *Proc. Hydraul. Eng.* **49** 391–6
[53] King J, Brown C and Sabet H 2003 A scenario-based holistic approach to environmental flow assessments for rivers *River Res. Appl.* **19** 619–39
[54] Fekete B M, Vörösmarty C J and Grabs W 2002 High-resolution fields of global runoff combining observed river discharge and simulated water balances *Glob. Biogeochem. Cycles* **16** 15-1–10
[55] Punjabi B and Johnson C A 2019 The politics of rural–urban water conflict in India: untapping the power of institutional reform *World Dev.* **120** 182–92
[56] Padowski J C and Gorelick S M 2014 Global analysis of urban surface water supply vulnerability *Environ. Res. Lett.* **9** 104004
[57] Scott C A, Flores-López F and Gastélum J R 2007 Appropriation of Río San Juan water by Monterrey City, Mexico: implications for agriculture and basin water sharing *Paddy Water Environ.* **5** 253–62
[58] Celio M, Scott C A and Giordano M 2010 Urban–agricultural water appropriation: the Hyderabad, India case *Geogr. J.* **176** 39–57
[59] FRESH AIR *et al* 2015 Drought in Calif. creates water wars between farmers, developers, residents (NPR) (available at: www.npr.org/2015/04/30/403283276/drought-in-calif-creates-water-wars-between-farmers-developers-residents) (Accessed 20 June 2022)
[60] Ofosu E, Van P, Giesen N and Odai S 2014 Success factors for sustainable irrigation development in Sub-Saharan Africa *Afr. J. Agric. Res.* **9** 3720–28
[61] Schmitt R J P, Rosa L and Daily G C 2022 Global expansion of sustainable irrigation limited by water storage *Proc. Natl Acad. Sci.* **119** e2214291119
[62] Shah T, van Koppen B, Merrey D J, De Lange M and Samad M 2002 Institutional alternatives in African smallholder irrigation: lessons from international experience with irrigation management transfer *Report No.:* 44563 (International Water Management Institute) (available at: https://econpapers.repec.org/paper/agsiwmirr/44563.htm) (Accessed 13 November 2023)
[63] Ali M H 2010 Fundamentals of irrigation development and planning *Fundamentals of Irrigation and On-farm Water Management* vol 1, ed M H Ali (Springer) pp 11–30
[64] Pathak R and Magliocca N R 2022 Assessing the representativeness of irrigation adoption studies: a meta-study of global research *Agriculture* **12** 2105
[65] Mekonnen M M and Hoekstra A Y 2012 A global assessment of the water footprint of farm animal products *Ecosystems* **15** 401–15
[66] Hutson S S, Barber N L, Kenny J F, Linsey K S, Lumia D S and Maupin M A 2004 *Estimated Use of Water in the United States in 2000* vol 1268 (Geological Survey (U.S.)) (available at http://pubs.er.usgs.gov/publication/cir1268)
[67] Schewe J *et al* 2014 Multimodel assessment of water scarcity under climate change *Proc. Natl Acad. Sci.* **111** 3245–50
[68] Gosling S N and Arnell N W 2016 A global assessment of the impact of climate change on water scarcity *Clim. Change* **134** 371–85
[69] DeAngelis A, Dominguez F, Fan Y, Robock A, Kustu M D and Robinson D 2010 Evidence of enhanced precipitation due to irrigation over the great plains of the United States *J. Geophys. Res. Atmos.* **115** D15115
[70] Xia W, Wang Y and Wang B 2022 Decreasing dust over the middle east partly caused by irrigation expansion *Earths Future* **10** e2021EF002252
[71] Douglas E M, Beltrán-Przekurat A, Niyogi D, Pielke R A and Vörösmarty C J 2009 The impact of agricultural intensification and irrigation on land–atmosphere interactions and Indian monsoon precipitation—a mesoscale modeling perspective *Glob. Planet. Change* **67** 117–28

[72] Condon L E and Maxwell R M 2019 Simulating the sensitivity of evapotranspiration and streamflow to large-scale groundwater depletion *Sci. Adv.* **5** eaav4574
[73] Seo S B, Mahinthakumar G, Sankarasubramanian A and Kumar M 2018 Conjunctive management of surface water and groundwater resources under drought conditions using a fully coupled hydrological model *J. Water Resour. Plan. Manage.* **144** 04018060
[74] Alcamo J, Henrichs T and Rosch T 2000 World water in 2025—Global modeling and scenario analysis for the world commission on water for the 21st century *Report No.: Report* A0002 (available at: https://web.archive.org/web/20070613043132/www.usf.uni-kassel.de/ftp/dokumente/kwws/kwws.2.pdf) (Accessed 2 February 2021) (https://doi.org/10.1126/sciadv.abc8259)
[75] Liu J *et al* 2017 Water scarcity assessments in the past, present, and future *Earths Future* **5** 545–59
[76] Veettil A V and Mishra A 2020 Water security assessment for the contiguous United States using water footprint concepts *Geophys. Res. Lett.* **47** e2020GL087061
[77] Giri S, Arbab N N and Lathrop R G 2018 Water security assessment of current and future scenarios through an integrated modeling framework in the Neshanic River Watershed *J. Hydrol.* **563** 1025–41
[78] Liu X, Liu W, Liu L, Tang Q, Liu J and Yang H 2021 Environmental flow requirements largely reshape global surface water scarcity assessment *Environ. Res. Lett.* **16** 104029
[79] Faralli M, Matthews J and Lawson T 2019 Exploiting natural variation and genetic manipulation of stomatal conductance for crop improvement *Curr. Opin. Plant Biol.* **49** 1–7
[80] Gonzalez-Dugo M P, Neale C M U, Mateos L, Kustas W P, Prueger J H, Anderson M C and Li F 2009 A comparison of operational remote sensing-based models for estimating crop evapotranspiration *Agric. For. Meteorol.* **149** 1843–53
[81] Gimpel J G, Lovin N, Moy B and Reeves A 2020 The urban–rural gulf in American political behavior *Polit Behav.* **42** 1343–68
[82] McDonald R I, Green P, Balk D, Fekete B M, Revenga C, Todd M and Montgomery M 2011 Urban growth, climate change, and freshwater availability *Proc. Natl Acad. Sci.* **108** 6312–7
[83] Blanc E, Strzepek K, Schlosser A, Jacoby H, Gueneau A, Fant C, Rausch S and Reilly J 2014 Modeling U.S. water resources under climate change *Earths Future* **2** 197–224
[84] Srinivasan V, Seto K C, Emerson R and Gorelick S M 2013 The impact of urbanization on water vulnerability: a coupled human–environment system approach for Chennai, India *Glob. Environ. Change* **23** 229–39
[85] Heidari H, Arabi M, Warziniack T and Kao S C 2021 Shifts in hydroclimatology of US megaregions in response to climate change *Environ. Res. Commun.* **3** 065002
[86] Ahn S and Sheng Z 2021 Assessment of water availability and scarcity based on hydrologic components in an irrigated agricultural watershed using SWAT *JAWRA J. Am. Water Resour. Assoc.* **57** 186–203
[87] Mukherjee S, Mishra A and Trenberth K E 2018 Climate change and drought: a perspective on drought indices *Curr. Clim. Change Rep.* **4** 145–63
[88] Nouri H, Stokvis B, Chavoshi Borujeni S, Galindo A, Brugnach M, Blatchford M L, Alaghmand S and Hoekstra A Y 2020 Reduce blue water scarcity and increase nutritional and economic water productivity through changing the cropping pattern in a catchment *J. Hydrol.* **588** 125086
[89] Davis K F, Chiarelli D D, Rulli M C, Chhatre A, Richter B, Singh D and DeFries R 2018 Alternative cereals can improve water use and nutrient supply in India *Sci. Adv.* **4** eaao1108
[90] Rathore L S, Aziz D, Demeke B W and Mekonnen M M 2023 Sustainability assessment of virtual water flows through cereal and milled grain trade among US counties *Environ. Res. Infrastruct. Sustain.* **3** 025001
[91] Vallino E, Ridolfi L and Laio F 2021 Trade of economically and physically scarce virtual water in the global food network *Sci. Rep.* **11** 22806
[92] Dalin C, Wada Y, Kastner T and Puma M J 2017 Groundwater depletion embedded in international food trade *Nature* **543** 700–4